JOURNAL OF VIROLOGY, May 1995, p. 2954–2961 Vol. 69, No. 5
0022-538X/95/$04.00+0

Poliovirus Infection Enhances the Formation of Two Ribonucleoprotein Complexes at the 3′ End of Viral Negative-Strand RNA

HOLGER H. ROEHL AND BERT L. SEMLER*

Department of Microbiology and Molecular Genetics, College of Medicine, University of California, Irvine, California 92717

Received 1 November 1994/Accepted 24 January 1995

To identify proteins involved in the formation of replication complexes at the 3′ end of poliovirus negative-strand RNA, a combined in vitro biochemical and in vivo genetic approach was used. Five subgenomic cDNA constructs were generated to transcribe different negative-strand RNA fragments. In UV cross-linking assays, distinct differences in binding of proteins in extracts from poliovirus-infected and uninfected cells to virus-specific, radiolabeled transcripts were observed. Two proteins present in extracts from poliovirus-infected cells with approximate molecular masses of 36 and 38 kDa were shown to cross-link to the 3′ end of poliovirus negative-strand RNA. Appearance of the 36- and 38-kDa proteins in UV cross-linking assays can be detected 3 to 3.5 h after infection, and cross-linking reaches maximum levels by 5 h after infection. The binding site for the 36-kDa protein overlaps with the computer-predicted loop b region of stem-loop I, the so-called cloverleaf structure, and the RNA sequence of this region is required for efficient binding. Transfection of full-length, positive-sense RNA containing a five-nucleotide substitution (positions 20 to 25) in the loop b region of stem-loop I into tissue culture cells yielded only viral isolates with a reversion at position 24 (U→C). This finding demonstrates that the wild-type cytidine residue at position 24 is essential for virus replication. RNA binding studies with transcripts corresponding to the 3′ end of negative-strand RNA suggest that complex formation with the 36-kDa protein plays an essential role during the viral life cycle.

Following entry of poliovirus (PV), the prototypic member of the *Picornaviridae*, into a permissive host cell, PV genomic RNA is replicated to generate full-length, intermediate negative-strand RNAs. New infectious positive-strand RNAs are subsequently produced by replication of the negative-strand RNAs. The virally encoded RNA-dependent RNA polymerase, $3D^{pol}$ (45), plays a key role in this replication process. However, in vitro, $3D^{pol}$ has been shown to nonspecifically replicate poly(A) RNA templates and nonviral, polyadenylated RNAs when provided with an oligo(U) primer (12, 29) or various host factor preparations (3, 9; for reviews, see references 30 and 37). This observation has led to the hypothesis that *cis*-acting sequences, located at the 3′ end of viral positive- and negative-strand RNAs, may interact with cellular and/or viral proteins, thus conferring specificity to the initiation step of viral RNA replication. Initiation of positive-strand RNA synthesis is presumably mediated by *cis*-acting sequences located at the 3′ end of negative-strand RNA, possibly in conjunction with sequences in the 5′ noncoding region (NCR) of positive-strand RNA (1, 2).

Previous studies investigating the initiation of positive-strand RNA synthesis in vitro were conducted by using membranous crude replication complexes isolated from PV-infected cells. Initiation of positive-strand RNA synthesis was shown to be supported by these crude replication complexes, and the 5′ ends of in vitro-synthesized RNA strands were identical to the VPg-linked termini of virion RNAs (40, 41). These early studies were hampered by the limitations of using crude extracts and by the lack of confirmatory genetic analyses. Several advances in experimental approaches have made it possible to unravel some of the molecular details of the initiation of positive-strand PV RNA synthesis. These include the ability to synthesize infectious PV RNA in vitro (18, 44), the evolution of biochemical techniques for studying RNA-protein interactions, and the development of cell-free systems for de novo poliovirus synthesis (4, 22). Indeed, some of these approaches were used to show that the first ~100 nucleotides (nt) of the PV genome, which form the so-called cloverleaf structure (31, 39), play an important role in viral RNA replication (2). The existence of this cloverleaf structure (also referred to as stem-loop I) at both the 5′ end of positive-strand RNAs and the 3′ end of negative-strand RNAs has been predicted by computer modeling (28). Biochemical evidence has also been obtained to support the existence of the cloverleaf at the 5′ end of positive-strand RNAs (2). The cloverleaf structure is subdivided into stem a and stem-loops b, c, and d (Fig. 1A). It has been reported that the cloverleaf structure is required for RNA replication initiation only on positive-strand RNA, and that a 36-kDa cellular protein together with the virally encoded 3CD protein interact with stem-loops b and d RNA, respectively (1, 2). A cellular 36-kDa protein, which also interacts with PV RNA in a complex with protein 3CD, has been identified as an N-terminal proteolytic fragment of a 50-kDa protein, eukaryotic elongation factor EF-1α (17). Whether these two 36-kDa proteins are identical is unknown. Other investigators have demonstrated the importance of stem-loop d for efficient PV type 3 RNA replication (33). Recently, it has been reported that viral RNA replication determinants also reside 3′ of the cloverleaf structure within a region containing sequences involved in translation initiation (5). The role of RNA-protein interactions at the 3′ end of negative-strand RNA in viral RNA replication, however, has not been elucidated.

To investigate the mechanism of initiation for PV positive-strand synthesis, we were interested in determining (i) what

* Corresponding author. Phone: (714) 824-7573. Fax: (714) 824-8598.

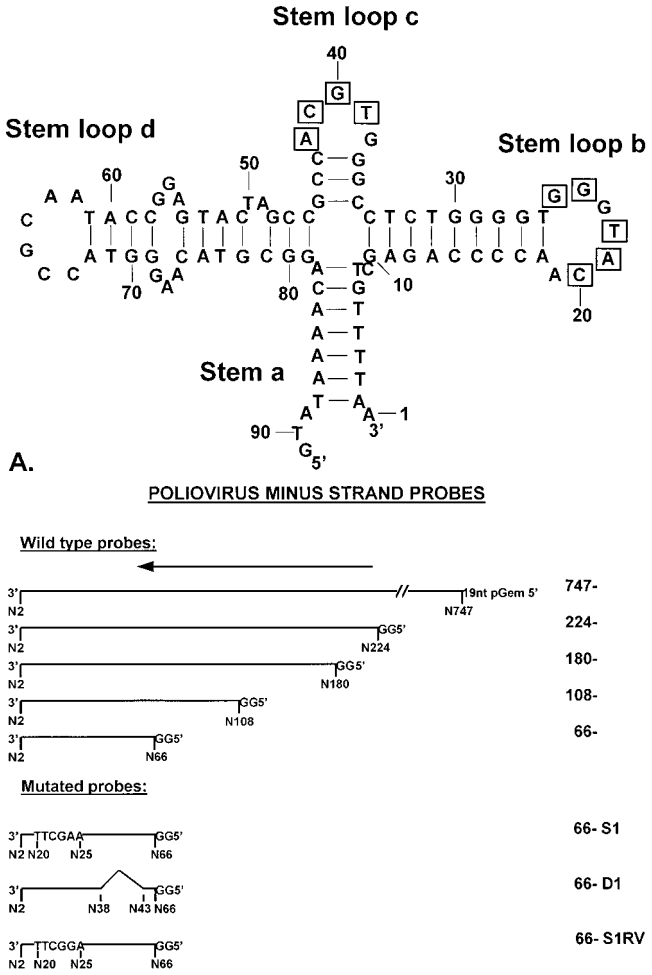

FIG. 1. Computer-predicted secondary structure of the 3′ end of PV negative-strand RNA and diagram of the RNA transcripts used in UV cross-linking assays. (A) A negative-strand RNA sequence complementary to nt 1 to 91 was used in the University of Wisconsin RNA FOLD program. The sequence shown is of negative polarity, but positive-strand numbers are used. The computer-predicted secondary structure is similar to the cloverleaf structure of stem-loop I described previously for PV positive-strand RNA. The cloverleaf structure consists of stem a and stem-loops b, c, and d. Nucleotides that were mutated in the loop b and loop c region are shown boxed. (B) PV cDNA fragments were subcloned into a T7-based transcription vector. RNA runoff transcripts (negative-strand polarity) were generated from plasmids linearized with *Mse*I (PV nt 1). The longest transcript, 747−, corresponds to the complement of the entire 5′ NCR. The next-shorter transcript, 224−, contains nt 224 to 2 (positive-strand numbers), 180− contains nt 180 to 2, 108− contains nt 108 to 2, and 66− contains nt 66 to 2. The 66− S1 transcript contains a 5-nt substitution in loop b (from nt 20 to 25) of stem-loop I, which does not perturb its computer-predicted secondary structure. The 66− D1 transcript contains a 4-nt deletion (nt 39 to 42) in loop c of stem-loop I. The 66− S1RV transcript is identical to 66− S1 except that the RNA has a guanosine residue (which is wild type and corresponds to a cytidine residue on the positive strand) at nt 24 instead of an adenosine residue.

cis-acting sequences at the 3′ end of negative-strand RNA are necessary for initiation and fidelity of positive-strand replication and (ii) what *trans*-acting factors of viral and/or host cell origin are required for initiation of positive-strand RNA replication. In an in vitro UV cross-linking assay, a distinct difference in binding of proteins to the 3′ end of PV negative-strand RNA was observed in extracts from PV-infected or uninfected cells. A 36-kDa and a 38-kDa protein present in extracts from PV-infected cells were shown to bind to the 3′ end of PV negative-strand RNA between positions 2 and 66 (note that positive-strand numbers are used, even though the transcripts are of negative polarity). These proteins are of cellular origin and appear to be modified or sequestered as a result of PV infection. UV cross-linking using PV RNA containing a 5-nt substitution (positions 20 to 25) in the loop b region of stem loop I showed that the binding site for the 36-kDa protein overlaps with the loop b region and that the primary RNA sequence of this region is required for efficient formation of a ribonucleoprotein complex. To correlate these in vitro results with viral RNA replication in vivo, full-length in vitro-transcribed genomic RNAs containing the 5-nt substitution (positions 20 to 25) in the loop b region were transfected into tissue culture cells. Only viral isolates with a reversion at position 24 (U→C) were recovered, demonstrating that the wild-type cytidine at position 24 is essential for virus replication. RNA binding studies with transcripts corresponding to the 3′ end of negative-strand RNA, together with the in vivo studies, suggest that complex formation with the 36-kDa protein plays an essential role during the viral life cycle.

MATERIALS AND METHODS

Construction of transcription templates. To generate RNA transcripts that have only two nonviral guanosine residues at their 5′ ends, the transcription vector pT747 (10) was modified by using two complementary synthetic oligonucleotides, HR1 (5′-AGCTTAGGCCTTATAGTGAGTCGTATTACAG-3′ [positive strand]) and HR2 (5′-CTG**TAATACGACTCACTATAAG**GCCTA-3′ [negative strand]). The annealed oligonucleotides contain both a *Hin*dIII and a *Pvu*II half site at their ends and contain the T7 promoter sequence (boldface sequence) followed by a *Stu*I recognition site (underlined sequence). The transcription vector pT747 was digested with *Hin*dIII (pGem2 nt 55) and *Pvu*II (pGem nt 98), and the 3.6-kb fragment was purified by agarose gel electrophoresis. The annealed oligonucleotides were then incubated together with the 3.6-kb pT747 fragment and T4 DNA ligase. The ligation mixture was transformed into competent *Escherichia coli* C600 cells, and colonies were screened for the plasmid pOT7N747-1. The integrity of this construct, as well as that of all constructs described below, was verified by sequencing across junctions of DNA fragments and/or the region containing introduced mutations, using the modified T7 DNA polymerase method (Sequenase; United States Biochemical).

To generate pT7N224−, plasmid pOT7N747-1 was digested with *Bam*HI (PV nt 220) and the resulting 5′ overhang was repaired. The plasmid was then digested with *Stu*I. The 2.6-kb fragment was purified by agarose gel electrophoresis and incubated with T4 DNA ligase. Competent cells were transformed with the ligation mixture and screened for pT7N224−. The RNAs transcribed from this plasmid (224−), as well as all the RNAs generated from transcription vectors described below, have only two G residues at their 5′ ends. Plasmid pT7N66− was constructed in a manner essentially identical to the approach used in constructing pT7N224−. The only modification was that the starting plasmid pOT7N747-1 was digested with *Kpn*I (PV nt 66) instead of *Bam*HI (PV nt 220).

To generate pT7N180−, plasmid pT7N224− was digested with *Nci*I (PV nt 178), and a 182-bp fragment containing PV nt 1 to 180 was purified by gel electrophoresis. The 5′ overhangs of the 180-bp fragment were repaired, and the fragment was then digested with *Kpn*I (PV nt 66). A 114-bp fragment containing PV nt 66 to 180 was purified by gel electrophoresis. Plasmid pOT7N747-1 was digested with *Stu*I and *Kpn*I (PV nt 66), and a 2,920-bp fragment was purified by gel electrophoresis. The 114- and 2,920-bp fragments were incubated together with T4 DNA ligase.

To generate pT7N108−, plasmid pT7N224− was digested with *Dde*I (PV nt 105, pGem nt 2689), and a 291-bp fragment containing PV nt 1 to 108 was purified by gel electrophoresis. The 5′ overhangs of the 291-bp fragment were repaired, and the fragment was then digested with *Eco*RI (pGem2 nt 10). A 112-bp fragment containing PV nt 1 to 108 was purified by gel electrophoresis. Plasmid pOT7N747-1 was digested with *Stu*I and *Eco*RI (pGem2 nt 10), and a 2,860-bp fragment was purified by gel electrophoresis. The 112- and 2,860-bp fragments were incubated together with T4 DNA ligase.

To generate pT7N66-S1, the following two complementary synthetic oligonucleotides were used: HRLOOPA+ (5′-AATTCTTAAAACAGCTCTGGGGTT**AAGCTT**ACCCCAGAGGCCCACG-3′ [positive strand]) and HRLOOPA− (5′-GGGCCTCTGGGGT**AAGCTT**AACCCCAGAGCTGTTTTAAG-3′ [negative strand]). The annealed oligonucleotides have both an *Eco*RI and a *Bgl*I half site at their ends and contain PV nt 1 to 19 and 26 to 40 or nt 26 to 37 (underlined sequence) interrupted by a *Hin*dIII recognition site (boldface sequence). This *Hin*dIII recognition site substitutes wild-type PV sequences (nt 20, 21, 22, 24, and 25) located in the loop a region of the computer-predicted cloverleaf structure. The transcription vector pT7N66− was subjected to a partial digestion with restriction endonucleases *Bgl*I (PV nt 35), and a 2,875-bp *Bgl*I fragment was

purified by agarose gel electrophoresis. The 2,875-bp *Bgl*I fragment was subsequently digested with *Eco*RI (pGem2 nt 10), and a 2,825-bp *Eco*RI-*Bgl*I fragment was purified by agarose gel electrophoresis. The annealed oligonucleotides HRLOOPA+ and HRLOOPA− were incubated together with the 2,825-bp *Eco*RI-*Bgl*I fragment and T4 DNA ligase.

To generate pT7N66-D1, plasmid pT7N66− was subjected to a partial digestion with *Bgl*I (PV nt 35), and a 2,875-bp *Bgl*I fragment was purified by agarose gel electrophoresis. The 3′ overhang was removed, and the 2,875-bp fragment was incubated with T4 DNA ligase.

Plasmid pPV1-5NC-S1 (encoding a full-length cDNA) was essentially constructed as described previously for pT7(τ)-PV1 (7). The only modification was in using the synthetic double-stranded oligonucleotides HRT2LOOPA (5′-CTGGGGTT**AAGCTT**ACCCCAGAGGCCCACG-3′ [positive strand]) and HRT2′LOOPA (5′-GGGCCTCTGGGGT**AAGCTT**AACCCCAGAGCT-3′ [positive strand]) instead of the double-stranded oligonucleotides containing a 3′ overhang of PV type 1 cDNA (nt 8 to 11) followed by PV type 1 cDNA from nt 12 to the *Bgl*I site at nt 35. HRT2LOOPA contains PV nt 12 to 19 and 26 to 40 interrupted by a *Hin*dIII recognition site (boldface sequence). HRT2′LOOPA contains PV nt 8 to 19 and 26 to 37 interrupted by a *Hin*dIII recognition site (boldface sequence). This *Hin*dIII recognition site substitutes wild-type PV sequences (nt 20, 21, 22, 24, and 25) located in the loop a region of the computer-predicted cloverleaf structure.

Construct pT7N66-S1RV was generated in a manner similar to that used for constructing pT7N66-S1, with the exception that two different synthetic oligonucleotides, HRLOOPA+RV (5′-AATTCTTAAAACAGCTCTGGGGTTAAGCCTACCCCAGAGGCCCACG-3′ [positive strand]) and HRLOOPA−RV (5′-GGGCCTCTGGGGTAGGCTTAACCCCAGAGCTGTTTTAAG-3′ [negative strand]) were used. These oligonucleotides differ from HRLOOPA+ and HRLOOPA− at one residue (underlined residue) within the substituted *Hin*dIII recognition site.

In vitro RNA transcription. In vitro transcriptions were carried out with bacteriophage T7 RNA polymerase (Pharmacia) as described previously (32). Constructs used as templates for transcription of RNAs corresponding to the 3′ end of PV negative-strand RNA were digested with *Mse*I (PV nt 1). Plasmid pGEM2, which was used for generating nonviral competitor RNA, was digested with *Rsa*I (pGem nt 2787). For generating wild-type and mutated full-length positive-strand RNA, plasmids pT7PV1 (15) and pPV1-5NC-S1, respectively, were linearized with *Eco*RI (PV nt ~7500).

Preparation of cellular extract. Cytoplasmic extracts from PV-infected and uninfected HeLa cells were prepared as described elsewhere (23, 35). Briefly, HeLa cells grown in suspension culture were harvested at various times (see Results) and washed three times in phosphate-buffered saline. Cells were then resuspended in an equal volume of lysis buffer (50 mM Tris [pH 8], 5 mM EDTA, 150 mM NaCl, 0.5% Nonidet P-40, 0.1 mM phenylmethylsulfonyl fluoride) and incubated for 20 min on ice. The mixture was centrifuged for 10 min at 12,000 × *g* at 4°C. Proteins contained in the supernatant were precipitated with 60% ammonium sulfate. The resulting pellet was resuspended in dialysis buffer (25 mM KCl, 5 mM HEPES [*N*-2-hydroxyethylpiperazine-N′-2-ethanesulfonic acid; pH 7.8], 2 mM $MgCl_2$, 0.1 mM EDTA [pH 8], 3.8% glycerol, 2 mM dithiothreitol, 0.1 mM phenylmethylsulfonyl fluoride) and dialyzed overnight against dialysis buffer containing an additional 10% glycerol. Extracts were frozen in aliquots at −70°C.

UV cross-linking assays. UV cross-linking assays were performed essentially as described previously (32). Typically, 5 pmol of ^{32}P-labeled RNA (1×10^6 to 8×10^6 cpm per reaction) was used per reaction, and the reaction mixtures were cross-linked at 254 nm for 20 min, using a Stratagene (La Jolla, Calif.) UV-Stratalinker. When appropriate, autoradiograms of UV cross-linked ribonucleoprotein complexes were scanned with a HP ScanJet II cx/T (Hewlett-Packard), and the intensity of bands was determined by using SigmaScan software.

Transfections of RNAs derived from wild-type and mutated full-length PV cDNAs. RNA transfections were performed by the DEAE-dextran procedure (19), with modifications described elsewhere (14). HeLa cell monolayers (90% confluent) in 60-mm-diameter dishes were transfected with 10, 1, and 0.1 μg of in vitro-transcribed full-length PV RNA derived from pPV1-5NC-S1 or 10 ng of in vitro-transcribed full-length PV RNA derived from pT7PV1 (15). Following transfection, cells were overlaid with liquid or semisolid agar medium and incubated at 33 or 37°C.

RNA and DNA sequencing. Viral RNA was prepared by extracting total cytoplasmic RNA from PV-infected cells, using the Nonidet P-40–sodium dodecyl sulfate (SDS) lysis method (6). Approximately 30 μg of total cytoplasmic RNA was used per sequencing reaction. A synthetic oligonucleotide complementary to PV nt 93 to 113 was annealed to the viral RNA and extended by using reverse transcriptase in the presence of [α-^{32}P]dATP, deoxynucleotides, and dideoxynucleotides (16, 34). Cesium chloride-purified plasmid DNA was sequenced by the modified T7 DNA polymerase method (Sequenase; United States Biochemical).

RESULTS

UV cross-linking of PV negative-strand RNAs, using extracts from uninfected and PV-infected cells. To investigate RNA-protein interactions at the 3′ end of PV type 1 negative-strand RNA, a nested series of cDNA constructs was generated and used as templates for the transcription of RNAs corresponding to the 3′ end of PV negative-strand RNA. The longest cDNA construct was used to transcribe the entire complement of the 5′ NCR (Fig. 1B) and contains computer-predicted stem-loops I through VI. The RNA generated from this construct is termed 747− (note that even though positive-strand numbers are used, the RNA is of negative-strand polarity). By using conveniently located restriction enzyme sites, successively shorter, 3′-coterminal constructs were generated. The RNA transcript called 224− contains the computer-predicted stem-loops I to III, 180− contains stem-loops I and II, 108− contains stem-loop I, the so-called cloverleaf structure, and the shortest transcript used, 66−, contains stem-loops b and c of the cloverleaf structure.

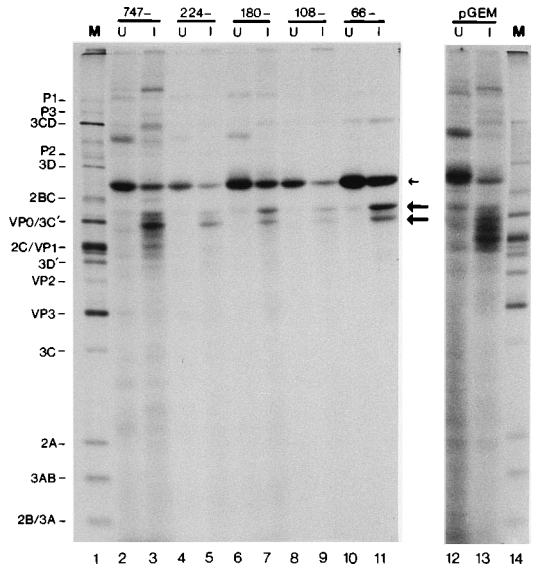

FIG. 2. UV cross-linking assays with PV negative-strand RNA probes, using extracts from uninfected and PV-infected HeLa cells. Portions (50 μg) of extract from either PV-infected or uninfected HeLa cells were used together with various ^{32}P-labeled RNA probes (5 pmol) in UV cross-linking assays. Following the cross-linking reactions, samples were boiled in Laemmli sample buffer and separated on an SDS–12.5% polyacrylamide gel. The 36- and 38-kDa protein bands are marked by large arrows; a nonspecific 50-kDa protein band is marked by a small arrow. Lanes: M, marker proteins ([^{35}S]Met labeled) from PV-infected HeLa cells; U, extract from uninfected cells; I, extract from PV-infected cells.

Extracts from uninfected and PV type 1-infected HeLa cells were prepared for UV cross-linking studies. It was determined that maximal amounts of PV positive-strand RNAs were present in infected cells at approximately 5 h after infection (data not shown). Subsequently, extracts from infected and uninfected cells were prepared at 5 h after infection. Extracts were then used with radiolabeled PV negative-strand probes in UV cross-linking assays (Fig. 2). A distinct difference in binding of proteins to the 3′ end of PV negative-strand RNAs in extracts from infected and uninfected cells was observed. Two major RNA-protein complexes specific to extracts from PV-infected cells were detected (bands marked by large arrows in Fig. 2). Their approximate molecular masses are 36 and 38 kDa. All of the PV-specific riboprobes tested appear to bind the same proteins, indicating that sequences and/or secondary structures located between positions 2 and 66 are sufficient for binding of these complexes. Pretreatment of extracts with proteinase K before UV cross-linking abolished the visualized bands (data not shown), indicating that they are indeed RNA-

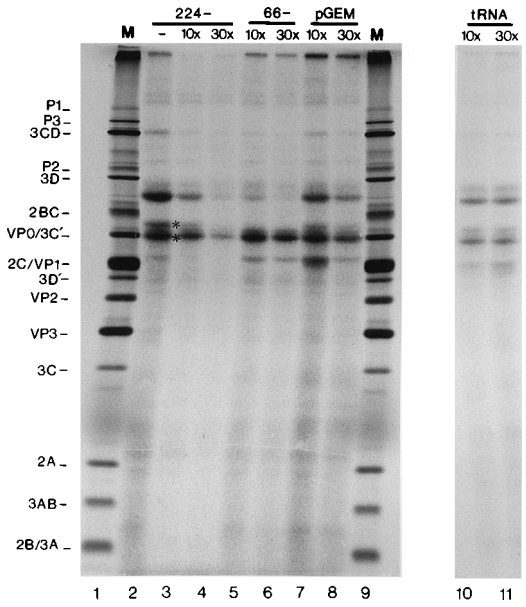

FIG. 3. UV cross-linking competition assays. UV cross-linking assays, using extract (50 μg) from PV-infected cells and radiolabeled 224− probe (5 pmol), were performed. Nonradioactive homologous (224− and 66−) and heterologous (pGEM and tRNA) competitor RNAs were added at either a 10- or 30-fold molar excess to the preincubation reaction. The 36- and 38-kDa protein bands are marked by asterisks. Lanes M, marker proteins ([^{35}S]Met labeled) from PV-infected HeLa cells.

protein complexes. A nonviral 144-nt RNA probe (lanes 12 and 13) formed these complexes with considerably less affinity than the viral probe. A protein of approximately 50 kDa (marked by a small arrow) was observed to bind to every RNA tested, i.e., RNAs of both viral as well as nonviral origin (data not shown). Because of its nonspecific UV cross-linking to RNA, the 50-kDa protein will not be discussed further.

To investigate the specificity of the 36- and 38-kDa protein complexes, UV cross-linking competition experiments using radiolabeled 224− RNA were performed (Fig. 3). Nonradioactive, homologous (224− and 66− RNAs) and heterologous (pGem and tRNA) competitor RNAs were added at either 10- or 30-fold molar excess to the preincubation reaction. Efficient competition for binding of both the 36- and 38-kDa protein (bands marked by asterisks) was observed when homologous competitor RNAs were used (lanes 3 to 6). Nonspecific, heterologous competitor RNAs did not compete efficiently for binding of the proteins (lanes 7, 8, 10, and 11), indicating that their binding to the 3′ end of PV negative-strand RNA is specific.

To determine whether the 36- and 38-kDa proteins were of viral or cellular origin, UV cross-linked RNA-protein complexes were used together with antibodies specific for PV VP1, VP2, VP3, 2C, 3AB, 3CD, 3C, and 3D in immunoprecipitation assays (data not shown). Neither the 36-kDa nor the 38-kDa protein was immunoprecipitated with any of the antibodies used, suggesting that both proteins are of host cell origin.

Properties of the 36- and 38-kDa protein-RNA complexes during PV infection. We were interested in determining at what time after PV infection interactions between the 36- and 38-kDa proteins with PV negative-strand RNA probes could be detected. Extracts were prepared from cells harvested at 30-min intervals following PV infection. These extracts were then used with radiolabeled 66− RNA in a UV cross-linking assay (Fig. 4). UV cross-linking of the 36- and 38-kDa proteins (marked by an arrow) was detected between 3 and 3.5 h after infection and reached maximum levels by 5 h after infection. The appearance of both cross-linked complexes between 3 and 3.5 h after infection correlates well with the time of maximal rates of viral RNA synthesis (3 to 4 h after infection) (8). This result suggests a role for both the 36- and 38-kDa protein complexes during viral RNA replication.

Several explanations could account for the observation that both RNA-protein complexes are not detectable in the first 3 h following infection. For example, it is possible that these proteins are newly synthesized during the course of infection. Alternatively, cellular proteins may be modified to have a higher affinity for PV RNA, or cellular proteins may be sequestered so that they become accessible during PV infection. To test the possibility that the 36- and 38-kDa proteins are synthesized de novo in response to PV infection, actinomycin D was added to HeLa cells at the time of infection to inhibit host cell transcription. Actinomycin D does not affect PV type 1 RNA replication (36). Cellular extract from actinomycin D-treated and untreated cells was prepared and used in a UV cross-linking assay (Fig. 5). In extracts from actinomycin D-treated cells, both RNA-protein complexes formed with an efficiency indistinguishable from that of extract from untreated cells. Since cap-dependent host cell protein translation ceases within 2 h following PV infection (11), this result suggests that the 36- and 38-kDa protein have already been synthesized at the time of infection and are modified or released from subcellular compartments as a result of infection. It is also possible, however, that both proteins are translated in a cap-independent manner (20, 24). Both wild-type PV type 1 replication and the appearance of the 36- and 38-kDa protein complexes are unaffected by actinomycin D, further supporting the conclusion that these proteins play a role in PV replication.

Binding site characterization of the 36- and 38-kDa protein by using mutated PV minus-strand probes. In Fig. 2, it was shown that both the 36- and 38-kDa proteins bind to negative-strand RNA sequences and/or secondary structures located between positions 2 and 66. Many RNA-binding proteins spe-

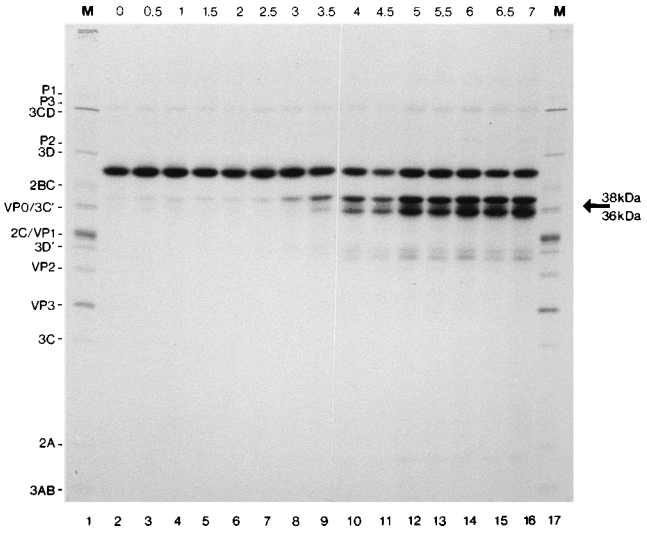

FIG. 4. UV cross-linking time course assay using extracts from PV-infected cells. Extracts were prepared following cell harvests at 30-min intervals after PV infection. UV cross-linking assays using 66− radiolabeled probe (5 pmol) and 50 μg of extract were performed. The 36- and 38-kDa proteins are marked by an arrow. Lanes M, marker proteins ([^{35}S]Met labeled) from PV-infected HeLa cells.

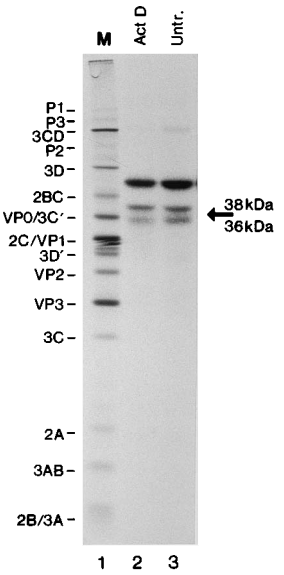

FIG. 5. UV cross-linking assays using extracts from PV-infected, actinomycin D-treated cells. Actinomycin D (5 μg/μl) was added to HeLa cells at the end of the PV adsorption period. UV cross-linking assays using extracts (50 μg) from actinomycin D-treated (Act D) and untreated (Untr.) PV-infected cells and radiolabeled 66− probe were performed. The 36- and 38-kDa proteins are marked by an arrow. Lane M, marker proteins ([^{35}S]Met labeled) from PV-infected HeLa cells.

cifically recognize single-stranded RNA regions such as loop structures of stem-loops or bulges (21). PV 66− RNA contains the computer-predicted stem-loops b and c of the cloverleaf structure. Therefore, our strategy was to mutate both loop regions. Two cDNA constructs were generated and used to synthesize two mutated PV negative-strand RNAs, 66− S1 and 66− D1 (Fig. 1). The 66− S1 transcript contains a 5-nt substitution in loop b (from positions 20 to 25) of stem-loop I. This substitution does not perturb the secondary structure of the 66− S1 transcript, which was predicted by using the University of Wisconsin FOLD program of Zuker and Stiegler (46). The 66− D1 transcript contains a 4-nt deletion (positions 39 to 42) in loop c of stem-loop I. These two mutated RNAs, together with wild type 66− RNA, were used in UV cross-linking assays to investigate the binding sites of the 36- and 38-kDa proteins (Fig. 6). All three RNA transcripts cross-linked to the 36- and 38-kDa proteins when incubated with increasing amounts of extracts from PV-infected cells. However, cross-linking of the 36-kDa protein is detectably decreased when the 66− S1 probe is used.

To quantitate the relative binding efficiencies of the two protein complexes to the different PV negative-strand-specific RNA probes, the intensities of the 36- and 38-kDa bands were determined by scanning autoradiograms. The ratio of the intensity of the 38-kDa band compared with the 36-kDa band was determined from a minimum of three independent experiments. Ratios were calculated to be 1.3 ± 0.3 for wild-type 66− RNA, 2.7 ± 0.8 for 66− S1 RNA, and 1.3 ± 0.5 for 66− D1 RNA. Both protein complexes were present at approximately equal amounts when the wild-type 66− or the 66− D1 probe was used. However, binding of the 36-kDa protein to the 66− S1 probe was only about one-third to one-half as efficient as to either the wild-type 66− or the 66− D1 probe. These results suggest that the binding site of the 36-kDa protein overlaps with the loop b region and that the primary nucleotide sequence of this region is important for efficient cross-linking. The sequence between positions 39 and 42 does not appear to be involved in the binding of these two proteins since it can be deleted without affecting cross-linking efficiency.

Characterization of the position 20 to 25 substitution mutation in vivo. To correlate the in vitro biochemical results of cellular proteins binding to the 3′ end of negative-strand RNAs to viral functions in vivo, the 5-nt substitution was introduced into a full-length PV cDNA clone (pPV1-5NC-S1). Full-length positive-strand RNA containing the substitution at positions 20 to 25 was generated by in vitro transcription and transfected into HeLa cells, and the cells were incubated at 33 or 37°C. Virus was recovered only at 33°C, and mutated RNAs were noninfectious at 37°C. The infectious virus recovered was designated Se1-5NC-S1. Four independent viral isolates were plaque purified, and passage 2 stocks were prepared. Plaques were slightly smaller than for wild-type virus, and titers were 0.5 to 0.7 log units lower than for wild-type virus (data not shown). Virion RNA from Se1-5NC-S1 was subjected to sequence analysis (Fig. 7), which revealed a U→C transition (reversion to wild type) at position 24. This U→C transition was found in all four independent viral isolates, suggesting that there is a strong selectional bias favoring this reversion to the wild-type sequence at position 24 and that the 5-nt substitution between positions 20 and 25 is lethal.

The viral isolates were then analyzed to investigate if the U→C transition had an effect on viral replication. All four viral isolates of Se1-5NC-S1, together with wild-type PV, were used to infect HeLa cells. Cells were harvested at various times after infection, and total RNA was isolated from these cells, transferred to a nitrocellulose membrane by slot blotting, and probed with radiolabeled synthetic oligonucleotides specific for positive- and negative-strand RNAs. The levels of both positive- and negative-strand RNAs in cells infected with any

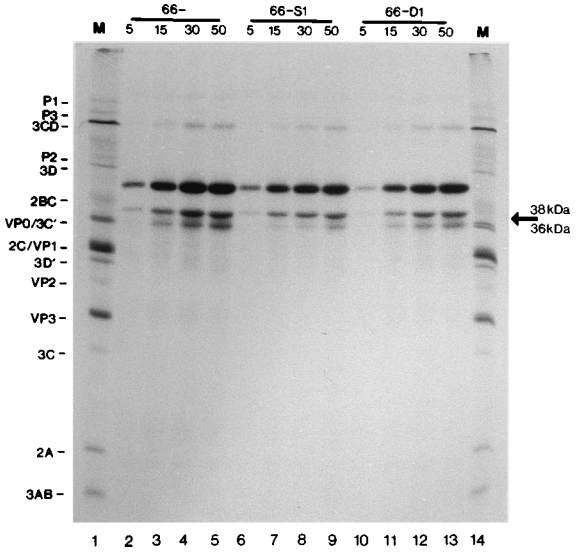

FIG. 6. UV cross-linking assays with extracts from PV-infected cells, using mutated PV negative-strand probes. UV cross-linking assays were performed with increasing amounts (5, 15, 30, and 50 μg) of extract from PV-infected cells. The following radiolabeled transcripts were used in this assay: 66−, which contains the PV wild-type sequence from positions 2 to 66 encompassing stem-loops b and c of the predicted cloverleaf structure; 66− S1, which has a 5-nt substitution (from positions 20 to 25) in loop b that does not affect its computer-predicted secondary structure; and 66− D1, which has a 4-nt deletion (positions 39 to 42) in stem-loop c (also see Fig. 1B). The 36- and 38-kDa proteins are marked by an arrow. Lanes M, marker proteins ([^{35}S]Met labeled) from PV-infected HeLa cells.

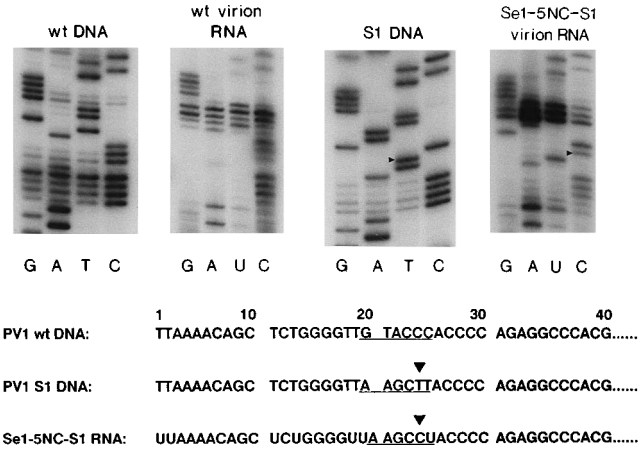

FIG. 7. Sequence analysis of wild-type and mutated PV cDNAs and virion RNAs. DNA and RNA were sequenced by the dideoxy-chain termination method. In the sequence shown below the autoradiograms, the site of the 5-nt substitution located between positions 20 and 25 is underlined. The arrowheads in both the autoradiogram and the sequence indicate the U→C transition at position 24. A cytidine residue is located at position 24 in wild-type (wt) PV RNA.

of the four viral isolates, which have reverted to a wild-type cytidine residue at position 24, do not differ significantly from those of wild-type PV (data not shown). This observation suggests that the wild-type cytidine residue at position 24 is essential for virus replication.

Relevance of a wild-type cytidine residue at position 24 for binding of the 36-kDa protein. We generated the cDNA construct 66− S1RV, which is identical to 66− S1 except that its RNA transcript has a guanosine residue (which is wild type and corresponds to a cytidine residue on the positive strand) at position 24 instead of an adenosine residue. To determine if this A→G transition (U→C transition on the positive strand) at position 24 would restore binding of the 36-kDa protein, UV cross-linking assays were performed with wild-type 66−, 66− S1, and 66− S1RV RNAs together with increasing amounts of extract form PV-infected cells (Fig. 8). The 36-kDa protein bound to 66− S1RV RNA at levels comparable to those of wild-type RNA. The binding of the 38-kDa protein to 66− S1RV RNA was slightly less than binding to 66− RNA, possibly because of an altered secondary structure of this mutated RNA. To quantitate the binding efficiency of the 36-kDa protein to 66− S1RV RNA, autoradiograms were scanned and the ratio of the 38-kDa band compared with the 36-kDa band was determined from a minimum of four independent experiments. Ratios were calculated to be 1.3 ± 0.3 for wild-type 66− RNA, 2.7 ± 0.8 for 66− S1 RNA, and 0.5 ± 0.2 for 66− S1RV RNA. Binding of the 36-kDa protein to 66− S1RV RNA was approximately twice as efficient as its binding to either the wild-type 66− or the 66− D1 RNA. This result suggests that a wild-type guanosine residue at position 24 is required for efficient binding of the 36-kDa protein. This finding, together with the in vivo results, is strongly indicative that binding of the 36-kDa protein to the 3′ end of negative-strand RNA plays an essential role during the viral life cycle.

DISCUSSION

The results presented in this study indicate that cellular proteins are involved in the formation of RNA replication initiation complexes at the 3′ end of PV negative-strand RNAs. Utilization of cellular proteins in the initiation of positive-strand and negative-strand RNA synthesis has been reported previously for Sindbis virus (25). The binding activity of proteins to the 3′ end of Sindbis negative-strand RNA was present in extracts from uninfected cells. The binding activity of both the 36- and 38-kDa proteins to the 3′ end of PV negative-strand RNA, although present at low levels in extracts from uninfected cells, is strongly increased in extracts from infected cells. This observation suggests that as a result of PV infection, cellular proteins are either newly synthesized, sequestered, or modified so that they have a higher affinity for binding to viral RNAs. A similar observation was recently reported for human rhinovirus 14 (42). The actinomycin D experiment presented in Fig. 5, together with the fact that cellular cap-dependent translation ceases within 2 h after infection, suggests that the appearance of the 36- and 38-kDa protein complexes between 3 to 3.5 h after infection is not due to de novo transcription and translation. While we cannot rule out the possibility that preexisting mRNAs encoding the 36- and 38-kDa proteins are translated in a cap-independent manner (20, 24), we favor the hypothesis that these two proteins are modified or released from a subcellular compartment in response to PV infection. It is possible, for example, that the 36- and 38-kDa proteins are products of proteolytic processing by viral proteinase 2A or 3C. The processed products, but not their precursor proteins, are recruited to play a role in the initiation and regulation of RNA replication.

Investigating RNA-protein interactions involved in replication at the 5′ end of positive-strand RNA, Andino et al. (1, 2) have reported binding of a 36-kDa cellular protein, present in extracts from uninfected cells, as a prerequisite for binding of poliovirus 3CD protein. Interestingly, this 36-kDa protein binds to the stem-loop b region of the cloverleaf structure on

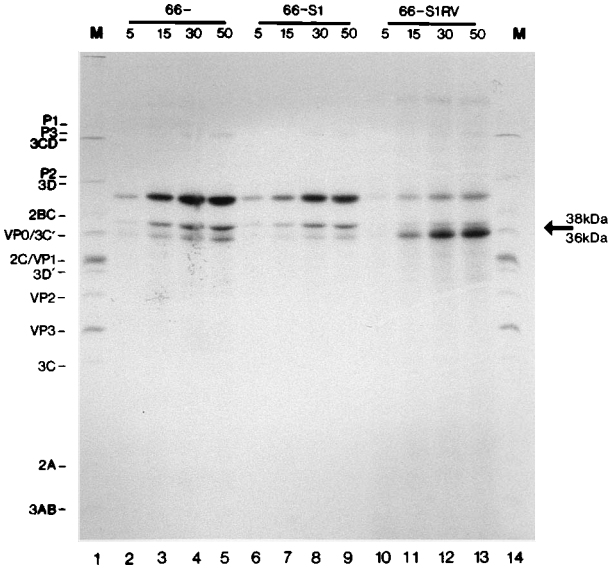

FIG. 8. UV cross-linking assays with extracts from PV-infected cells, using mutated PV negative-strand probes. UV cross-linking assays were performed with increasing amounts (5, 15, 30, and 50 μg) of extract from PV-infected cells. The following radiolabeled transcripts were used in this assay: 66−, which contains the PV wild-type sequence from positions 2 to 66 encompassing stem-loops b and c of the predicted cloverleaf structure; 66− S1, which has a 5-nt substitution in loop b (from positions 20 to 25) that does not affect its computer-predicted secondary structure; and 66− S1RV, which is identical to 66− S1 except that the RNA has a guanosine residue (which is wild type and corresponds to a cytidine residue on the positive strand) at position 24 instead of an adenosine residue (also see Fig. 1B). The 36- and 38-kDa proteins are marked by an arrow. Lanes M, marker proteins ([^{35}S]Met labeled) from PV-infected HeLa cells.

positive-strand RNA, and a wild-type cytidine residue at position 24 is also important for its binding. Identification of a 36-kDa protein (p36) which interacts with purified 3CD protein and also binds to the cloverleaf structure on positive-strand RNA was described recently (17). It was determined that this p36 is an N-terminal proteolytic fragment of p50, the eukaryotic elongation factor EF-1α. Harris et al. (17) suggested that viral protein 3AB could substitute for p36 in forming a complex with 3CD that then binds to the cloverleaf structure on positive-strand RNA. We have not observed binding of viral protein 3CD or 3AB to the 3′ end of negative-strand RNA, but it is possible that this is due to differences in the experimental setup. It is not known whether the 36-kDa protein described in this report is identical to the p36 protein described by Andino et al. (1, 2) or Harris et al. (17). It is conceivable that a 36-kDa protein(s) has baseline levels of affinity for a similar region on positive- as well as negative-strand RNA and that this region of the RNA forms a duplex in vivo, thus constituting a high-affinity binding site.

Using full-length PV RNA transcripts containing a substitution at positions 20 to 25 for in vivo studies, we determined that a wild-type cytidine residue at position 24 is important for viral replication. Even though sequences necessary for internal ribosome entry (IRES) have been mapped between PV positions 200 to 600 (14, 26, 27, 43), it is possible that the substitution at positions 20 to 25 exerts its effect during translation initiation and not during RNA replication. It has been reported that a 6-nt insertion at position 21 results in a defect in viral translation (38). This 6-nt insertion, unlike our 5-nt substitution, perturbs the computer-predicted secondary structure of the 5′ end of positive-strand RNA and could therefore influence higher-order structures within the IRES region necessary for translation initiation. The translation efficiencies of full-length PV RNAs containing the 5-nt substitution or wild-type sequences between positions 20 and 25 were indistinguishable, as judged by in vitro translation assays (data not shown). This result, together with the fact that all IRES elements have been mapped 3′ of the cloverleaf structure, leads us to rule out the possibility that the substitution at positions 20 to 25 affects PV translation.

Using a series of PV type 3 replicons in in vivo experiments, Rohll et al. (33) showed the importance of an adenosine or cytidine residue at position 24 and a cytidine residue at position 25 for efficient viral replication. This observation is in agreement with our finding that a wild-type cytidine residue at position 24 is essential for viral replication of PV type 1. These same investigators also showed that stem-loop d (positions 46 to 81) of the cloverleaf structure contains major replication determinants. A recent report by Borman et al. (5) suggests that replication signals may also reside within the PV IRES region. Even though we have not detected protein binding to the corresponding regions of negative-strand RNA, a fully functional replication initiation element may consist of several independent domains which are actually in close proximity to each other in vivo due to RNA tertiary structure. In addition, it is possible that in vivo, replication initiation complexes assemble on duplex RNA formed by partial hybridization of positive- and negative-strand RNAs, as has been suggested for coronavirus replication (13). Such a mechanism could account for the observed formation of putative replication complexes involving the 5′ NCR of positive-strand RNA that, when complexed with complementary negative-strand intermediate RNAs, would allow transfer of the initiation complex to the appropriate template sequences that will ultimately direct the synthesis of nascent, positive-strand progeny RNAs.

ACKNOWLEDGMENTS

We are indebted to Don Summers for suggesting the actinomycin D experiment and Stacey Stewart for help in constructing plasmid pPV1-5NC-S1. We thank Hung Nguyen and Hanh Le for expert technical assistance, Stephen Todd for critical review of the manuscript, and Eckard Wimmer for communication of data prior to publication.

H.H.R. is the recipient of American Cancer Society postdoctoral fellowship PF 3756. This work was supported by Public Health Service grant AI 22693 from the National Institutes of Health.

REFERENCES

1. **Andino, R., G. E. Rieckhof, P. L. Achacoso, and D. Baltimore.** 1993. Poliovirus RNA synthesis utilizes an RNP complex formed around the 5′-end of viral RNA. EMBO J. **12:**3587–3598.
2. **Andino, R., G. E. Rieckhof, and D. Baltimore.** 1990. A functional ribonucleoprotein complex forms around the 5′ end of poliovirus RNA. Cell **63:**369–380.
3. **Baron, M. H., and D. Baltimore.** 1982. Purification and properties of a host cell protein required for poliovirus replication in vitro. J. Biol. Chem. **257:** 12351–12358.
4. **Barton, D. J., and J. B. Flanegan.** 1993. Coupled translation and replication of poliovirus RNA in vitro: synthesis of functional 3D polymerase and infectious virus. J. Virol. **67:**822–831.
5. **Borman, A. M., F. G. Deliat, and K. M. Kean.** 1994. Sequences within the poliovirus internal ribosome entry segment control viral RNA synthesis. EMBO J. **13:**3149–3157.
6. **Campos, R., and L. P. Villarreal.** 1982. An SV40 deletion mutant accumulates late transcripts in a paranuclear extract. Virology **119:**1–11.
7. **Charini, W. A., C. C. Burns, E. Ehrenfeld, and B. L. Semler.** 1991. *trans* rescue of a mutant poliovirus RNA polymerase function. J. Virol. **65:**2655–2665.
8. **Darnell, J. E., M. Girard, D. Baltimore, D. F. Summers, and J. V. Maizel.** 1967. The synthesis and translation of poliovirus RNA, p. 375–401. *In* J. S. Colter and W. Paranchych (ed.), The molecular biology of viruses. Academic Press, New York.
9. **Dasgupta, A., P. Zabel, and D. Baltimore.** 1980. Dependence of the activity of the poliovirus replicase on a host cell protein. Cell **19:**423–429.
10. **Dildine, S. L., and B. L. Semler.** 1992. Conservation of RNA-protein interactions among picornaviruses. J. Virol. **66:**4364–4376.
11. **Ehrenfeld, E.** 1984. Picornavirus inhibition of host cell protein synthesis, p. 177–221. *In* H. Fraenkel-Conrat and R. R. Wagner (ed.), Comprehensive virology, vol. 19. Plenum Press, New York.
12. **Flanegan, J. B., and D. Baltimore.** 1977. Poliovirus-specific primer-dependent RNA polymerase able to copy poly(A). Proc. Natl. Acad. Sci. USA **74:**3677–3680.
13. **Furuya, T., and M. M. C. Lai.** 1993. Three different cellular proteins bind to complementary sites on the 5′-end-positive and 3′-end-negative strands of mouse hepatitis virus RNA. J. Virol. **67:**7215–7222.
14. **Haller, A. A., J. H. C. Nguyen, and B. L. Semler.** 1993. Minimum internal ribosome entry site required for poliovirus infectivity. J. Virol. **67:**7461–7471.
15. **Haller, A. A., and B. L. Semler.** 1992. Linker scanning mutagenesis of the internal ribosome entry site of poliovirus RNA. J. Virol. **66:**5075–5086.
16. **Hamlyn, D. H., G. G. Brownlee, C. C. Cheng, M. J. Gait, and C. Milstein.** 1978. Complete sequence of constant 3′ noncoding regions on an immunoglobulin mRNA using the dideoxy nucleotide method of RNA sequencing. Cell **15:**1067–1075.
17. **Harris, K. S., W. Xiang, L. Alexander, W. S. Lane, A. V. Paul, and E. Wimmer.** 1994. Interaction of poliovirus polypeptide $3CD^{pro}$ with the 5′ and 3′ termini of the poliovirus genome: identification of viral and cellular cofactors needed for efficient binding. J. Biol. Chem. **269:**27004–27014.
18. **Kaplan, G., J. Lubinski, A. Dasgupta, and V. R. Racaniello.** 1985. *In vitro* synthesis of infectious poliovirus RNA. Proc. Natl. Acad. Sci. USA **82:**8424–8428.
19. **LaMonica, N., C. Meriam, and V. R. Racaniello.** 1986. Mapping of sequences required for mouse neurovirulence of poliovirus type 2 Lansing. J. Virol. **57:**515–525.
20. **Macejak, D. G., and P. Sarnow.** 1991. Internal initiation of translation mediated by the 5′ leader of a cellular mRNA. Nature (London) **353:**90–94.
21. **Mattaj, I. W.** 1993. RNA recognition: a family matter? Cell **73:**837–840.
22. **Molla, A., A. V. Paul, and E. Wimmer.** 1991. Cell-free, de novo synthesis of poliovirus. Science **254:**1647–1651.
23. **Najita, L., and P. Sarnow.** 1990. Oxidation-reduction sensitive interaction of a cellular 50-kDa protein with an RNA hairpin in the 5′ noncoding region of the poliovirus genome. Proc. Natl. Acad. Sci. USA **87:**5846–5850.
24. **Oh, S. K., M. P. Scott, and P. Sarnow.** 1992. Homeotic gene antennapedia mRNA contains 5′-noncoding sequences that confer translational initiation by internal ribosome binding. Genes Dev. **6:**1643–1653.
25. **Pardigon, N., and J. H. Strauss.** 1992. Cellular proteins bind to the 3′ end of Sindbis virus minus-strand RNA. J. Virol. **66:**1007–1015.

26. **Pelletier, J., G. Kaplan, V. R. Racaniello, and N. Sonenberg.** 1988. Cap-independent translation of poliovirus mRNA is conferred by sequence elements within the 5′ noncoding region. Mol. Cell. Biol. **8:**1103–1112.
27. **Pelletier, J., and N. Sonenberg.** 1988. Internal initiation of translation of eukaryotic mRNA directed by a sequence derived from poliovirus RNA. Nature (London) **334:**320–325.
28. **Pilipenko, E. V., S. V. Maslova, A. N. Sinyakov, and V. I. Agol.** 1992. Towards identification of cis-acting elements involved in the replication of enterovirus and rhinovirus RNAs: a proposal for the existence of tRNA-like terminal structures. Nucleic Acids Res. **20:**1739–1745.
29. **Plotch, S. J., O. Palant, and Y. Gluzman.** 1989. Purification and properties of poliovirus RNA polymerase expressed in *Escherichia coli*. J. Virol. **63:** 216–225.
30. **Richards, O. C., and E. Ehrenfeld.** 1990. Poliovirus RNA replication. Curr. Top. Microbiol. Immunol. **161:**89–119.
31. **Rivera, R., J. D. Welch, and J. V. Maizel.** 1988. Comparative sequence analysis of the 5′ noncoding region of the enteroviruses and rhinoviruses. Virology **165:**42–50.
32. **Roehl, H. H., and B. L. Semler.** 1994. In vitro biochemical methods for investigating RNA-protein interactions in picornaviruses, p. 169–182. *In* K. W. Adolph (ed.), Methods in molecular genetics, vol. 4. Academic Press, Inc., Orlando, Fla.
33. **Rohll, J. B., N. Percy, R. Ley, D. J. Evans, J. W. Almond, and W. S. Barclay.** 1994. The 5′-untranslated regions of poliovirus RNAs contain independent functional domains essential for RNA replication and translation. J. Virol. **68:**4384–4391.
34. **Sanger, F., S. Nicklen, and A. R. Coulson.** 1977. DNA sequencing with chain-terminating inhibitors. Proc. Natl. Acad. Sci. USA **74:**5463–5467.
35. **Sarnow, P.** 1989. Translation of glucose-regulated protein 78/immunoglobulin heavy-chain binding protein mRNA is increased in poliovirus-infected cells at a time when cap-dependent translation of cellular mRNAs is inhibited. Proc. Natl. Acad. Sci. USA **86:**5795–5799.
36. **Schaffer, F. L., and M. Gordon.** 1966. Differential inhibitory effects of actinomycin D among strains of poliovirus. J. Bacteriol. **91:**2309–2316.
37. **Semler, B. L., R. J. Kuhn, and E. Wimmer.** 1988. Replication of the poliovirus genome, p. 23–48. *In* E. Domingo, J. J. Holland, and P. Ahlquist (ed.), RNA genetics, vol. 1. CRC Press, Inc., Boca Raton, Fla.
38. **Simoes, E. A. F., and P. Sarnow.** 1991. An RNA hairpin at the extreme 5′ end of the poliovirus RNA genome modulates viral translation in human cells. J. Virol. **65:**913–921.
39. **Skinner, M. A., V. R. Racaniello, G. Dunn, J. Cooper, P. D. Minor, and J. W. Almond.** 1989. New model for the secondary structure of the 5′ non-coding RNA of poliovirus is supported by biochemical and genetic data that also show that RNA secondary structure is important in neurovirulence. J. Mol. Biol. **207:**379–392.
40. **Takeda, N., R. J. Kuhn, C. F. Yang, T. Takegami, and E. Wimmer.** 1986. Initiation of poliovirus plus-strand RNA synthesis in a membrane complex in infected HeLa cells. J. Virol. **60:**43–53.
41. **Takegami, T., R. J. Kuhn, C. W. Anderson, and E. Wimmer.** 1983. Membrane-dependent uridylylation of the genome-linked protein of poliovirus. Proc. Natl. Acad. Sci. USA **80:**7447–7451.
42. **Todd, S., J. H. C. Nguyen, and B. L. Semler.** RNA-protein interactions directed by the 3′ end of human rhinovirus genomic RNA. J. Virol., in press.
43. **Trono, D., R. Andino, and D. Baltimore.** 1988. An RNA sequence of hundreds of nucleotides at the 5′ end of poliovirus RNA is involved in allowing viral protein synthesis. J. Virol. **62:**2291–2299.
44. **van der Werf, S., J. Bradley, E. Wimmer, F. W. Studier, and J. J. Dunn.** 1986. Synthesis of infectious poliovirus RNA by purified T7 RNA polymerase. Proc. Natl. Acad. Sci. USA **83:**2330–2334.
45. **Van Dyke, T. A., and J. B. Flanegan.** 1980. Identification of poliovirus p63 as a soluble RNA-dependent RNA polymerase. J. Virol. **35:**732–740.
46. **Zuker, M., and P. Stiegler.** 1981. Optimal computer folding of large RNA sequences using thermodynamics and auxiliary information. Nucleic Acids Res. **9:**133–148.